Published in final edited form as:
Free Radic Biol Med. 2012 February 1; 52(3): 616–625. doi:10.1016/j.freeradbiomed.2011.10.496.

The reaction of HOCl and cyanocobalamin: corrin destruction and the liberation of cyanogen chloride

Husam M. Abu-Soud[a,d,*], **Dhiman Maitra**[a], **Jaeman Byun**[b], **Carlos Eduardo A. Souza**[a], **Jashoman Banerjee**[a], **Ghassan M. Saed**[a], **Michael P. Diamond**[a], **Peter R. Andreana**[c], and **Subramaniam Pennathur**[b,*]

[a]Departments of Obstetrics and Gynecology The C.S. Mott Center for Human Growth and Development Wayne State University School of Medicine, Detroit, MI 48201, USA

[b]Division of Nephrology, Department of Internal Medicine, University of Michigan Medical School, Ann Arbor, MI 48109, USA

[c]Department of Chemistry, Wayne State University, Detroit, MI 48202, USA

[d]Department of Biochemistry and Molecular Biology, The C.S. Mott Center for Human Growth and Development, Wayne State University School of Medicine, Detroit, MI 48201, USA

Abstract

Overproduction of hypochlorous acid (HOCl) has been associated with the development of variety of disorders such as inflammation, heart disease, pulmonary fibrosis and cancer through its ability to modify different biomolecules. HOCl is a potent oxidant generated by the myeloperoxidase-hydrogen peroxide-chloride system. Recently, we have provided evidence to support the important link between higher levels of HOCl with heme destruction and free iron release from hemoglobin and RBCs. Our current finding extend this work and show the ability of HOCl to mediate the destruction of metal-ion derivatives of tetrapyrrole macrocyclic rings, such as cyanocobalamin (Cobl) a common pharmacological form of vitamin B12. Cyanocobalamin is a water soluble vitamin which plays an essential role as an enzyme cofactor and antioxidant, modulating nucleic acid metabolism and gene regulation. It is widely used as a therapeutic agent and supplement, because of its efficacy and stability. In this report, we demonstrate that while Cobl can be an excellent antioxidant, exposure to high levels of HOCl can overcome the beneficial effects of Cobl and generate proinflammatory reaction products. Our rapid kinetic, HPLC and mass spectrometric analyses showed that HOCl can mediate corrin ring destruction and liberate cyanogen chloride (CNCl) through a mechanism that initially involves α-axial ligand replacement in Cobl to form a chlorinated derivative, hydrolysis, and cleavage of the phosphor-nucleotide moiety. Additionally, it can liberate free Co which can perpetuate metal-ion induced oxidant stress. Taken together, this is the first report of generation of toxic molecular products through the interaction of Cobl with HOCl.

*Address Correspondence to Husam M. Abu-Soud, Ph.D., Wayne State University School of Medicine, Department of Obstetrics and Gynecology, The C.S. Mott Center for Human Growth and Development, 275 E. Hancock, Detroit, MI 48201, Tel: 313 577-6178; Fax: 313 577-8554; habusoud@med.wayne.edu.

Keywords

Free cobalt; vitamin B12 deficiency; vitamin B12 degradation; mammalian peroxidases; mass spectrometry; oxidative stress; corrin; porphyrin; stopped-flow; inflammation; aging; free metal toxicity; cyanogens chloride

INTRODUCTION

HOCl is a potent oxidant generated by myeloperoxidase (MPO), a neutrophil-derived heme peroxidase that uses hydrogen peroxide (H_2O_2) and chloride (Cl^-) as co-substrates [1]. HOCl plays an important role in the innate immune system by oxidatively destroying invading pathogens and microbes. However, sustained high levels of HOCl may cause host tissue injury in acute and chronic inflammatory conditions [2]. Activated neutrophils have been reported to generate around 150–425 μM of HOCl per hour [3, 4]. It is estimated that HOCl levels reach about 5 mM at sites of inflammation [5]. Indeed, high level of HOCl has been implicated in development and progression of a number of pathological conditions such as vasculitis, atherosclerosis, pulmonary fibrosis, diabetic complications, glomerulonephritis, cancer and even oocyte ageing [6–9]. HOCl also causes protein chlorination [10] and protein aggregation [11] which have been demonstrated in neurodegenerative disorders such as in amyloid plaques and Parkinson's disease [12–14]. HOCl can react with cyanide (CN^-) to generate an extremely toxic compound, cyanogen chloride (CNCl), which in turn is hydrolyzed by water to produce hydrogen cyanide (HCN) [15].

CNCl is a volatile and toxic asphyxiant that can affect multiple organs such as the central nervous, cardiovascular and pulmonary systems[16]. It is an extremely labile molecule and its toxicity in biological system lies in its ability to release CN^- through its reaction with sulfhydryl compounds such as GSH and protein thiols [17]. The liberated CN^- can in turn inhibit mitochondrial cytochrome oxidase [18] and hence block electron transport, resulting in decreased oxidative metabolism and oxygen utilization, a fatal process for an organism.

Vitamin B12 is an important water-soluble vitamin which regulates red blood cell and neural cell activity and displays antioxidant properties [19, 20]. Deficiency of this vitamin has been associated with megaloblastic anemia and cognitive dysfunction in neurodegenerative disorders including Parkinson's and Alzheimer's disease [21]. Cyanocobalamin (Cobl) is the most common supplemental form of vitamin B12. Cyanocobalamin at doses of 100 to 1000 μg, are commonly prescribed for subjects with deficiency of the vitamin in conditions such as pernicious anemia[22]. Cobl is produced from hydroxocobalamin, naturally produced by bacteria, and used in all natural products. In the process of purification and separation of hydroxocobalamin from bacteria through charcoal (a substance rich with cyanide) columns, hydroxocobalamin changes to cyanocobalamin form. Cobl's structure is mainly based on a corrin ring, which is similar to the porphyrin moiety found in hemoproteins with two pyrrole rings attached directly to each other and a Co atom residing in the center. Four of the six coordination sites of Co atom are the pyrroyle nitrogen atoms provided by the corrin ring, and a fifth is a nitrogen of the 5,6- dimethylbenzimidazole group at the lower (or α-) axial ligand (Fig. 1) [23]. The other nitrogen of the 5,6-dimethylbenzimidazole is linked to a five-carbon sugar, which in turn connects to a phosphate group, and then back onto the corrin ring via one of the seven-amide groups attached to the periphery of the corrin ring. The sixth coordination site, known as the center of reactivity, is the upper/β-axial ligand occupied by a cyano group (-CN). These characteristic features make the corrin ring more flexible and less flat compared to the porphyrin ring.

Recently we have demonstrated that HOCl can oxidatively cleave the heme moiety from hemoglobin and free heme to release free iron [24, 25]. In this work we extended our observation to Cobl, a similar corrin macrocyclic compound. Our results for the first time show that HOCl can mediate destruction of the corrin ring of Cobl, through a mechanism that involves disruption of axial coordination of the Co atom and cleavage of the corrin ring. The liberated CN^- reacts with HOCl and generates CNCl.

MATERIALS AND METHODS

Materials

All the materials used were of highest purity grade and used without further purification. Sodium hypochlorite (NaOCl), pyridine, 1,3 dimethyl barbituric acid, Cobl, L-methionine, methanol- HPLC grade, were obtained from Sigma Aldrich (St. Louis, MO, USA).

Absorbance Measurements

The absorbance spectra was recorded using a Cary 100 Bio UV–visible spectrophotometer, at 25 °C, pH 7.0. Experiments were performed in a 1-ml phosphate buffer solution (200 mM, pH 7.4) supplemented with fixed amount of Cobl (11 μM) and increasing concentration of HOCl (0, 100, 200, 300, 400, 500, 600, 1000 μM). After 2 hours incubation for reaction completion, methionine (5-fold of the final HOCl concentration) was added to eliminate excess HOCl and absorbance changes were recorded from 300 to 700 nm.

Rapid Kinetic Measurements

The kinetic measurements of HOCl-mediated Cobl destruction were performed using a dual syringe stopped-flow instrument obtained from Hi-Tech, Ltd. (Model SF-61). Measurements were carried out under an aerobic atmosphere at 25°C following rapid mixing of equal volumes of a buffer solution contains fixed amount of Cobl (22 μM) and a buffer solution containing increasing concentration of HOCl. The time course of the absorbance change was fitted to a single-exponential (Eq. 1), or a double-exponential (Eq. 2) function as indicated. Signal-to-noise ratios for all kinetic analyses were improved by averaging at least six to eight individual traces. In some experiments, the stopped-flow instrument was attached to a rapid scanning diode array device (Hi-Tech) designed to collect multiple numbers of complete spectra (200–800 nm) at specific time ranges. The detector was automatically calibrated relative to a holmium oxide filter, as it has spectral peaks at 360.8, 418.5, 446.0, 453.4, 460.4, 536.4, and 637.5 nm, which were used by the software to correctly align pixel positions with wavelength.

$$Y = 1 - e^{-kt} + C \quad \text{Eq. 1}$$

$$Y = Ae^{-k_1 t} + Be^{-k_2 t} + C \quad \text{Eq. 2}$$

High Performance Liquid Chromatography (HPLC) analysis

HPLC analyses was carried out using a Shimadzu HPLC system equipped with a SCL-10A system controller, with a binary pump solvent delivery (LC-10 AD) module and a SIL-10AD auto-injector connected to a SPD-M10A diode array detector (DAD) and a RF-10A XL fluorescence detector. Alltech 5 μm particle size, 4.6 × 150 mm reverse-phase octadecylsilica (C18) HPLC column was used. The photodiode array detector was set at 360 nm to monitor the chromatogram. The column was eluted at a flow rate of 1.0 mL/min with linear gradients of solvents A and B (A, water; B, methanol). The solvent gradient was as

follows: 0 to 15 min, 20–85% B; 15 to 20 min, 85% B; then the solvent B composition dropped down to 20% within 21 min and the column was equilibrated at 20% solvent B for 25 min. After treatment of Cobl with HOCl, 50 μL of the reaction mixture was injected. Each sample was analyzed in triplicate.

Colorimetric detection of CNCl

CNCl was detected colorimetrically using the pyridine-1,3 dimethyl barbituric acid reagent [26]. In this assay, CNCl reacts with pyridine to form a dialdehyde, Glutacon dialdehyde, which then reacts with 1,3 dimethyl barbituric acid and condenses to form a violet colored polymethine dye (Eq. 3). The composition of the pyridine-1,3, dimethyl barbituric acid (coloring reagent) was as follows. 1.2 g of 1, 3 dimethyl barbituric acid was dissolved in a mixture of 12.8 mL of water and 6 mL of pyridine, and then 1.2 mL of HCl was added to the solution to bring the total volume to 20 mL. 500 μL of coloring reagent was added to 500 μL of cyanocobalamin-HOCl reaction mixture and was incubated for 15 minutes at 10°C. The absorbance of the resulting violet-colored solution was measured at 587.5 nm against cyanocobalamin-HOCl reaction mixture (without addition of coloring reagent, but diluted with equal volume of water) to substract the absorbance due to residual cyanocobalamine. The amount of CNCl was determined from the extinction coeffcient of $1.03 \times 10^5\ M^{-1}cm^{-1}$ for the violet colored complex [27].

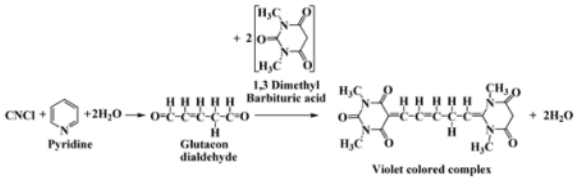

Eq. 3

Treatment of Cobl with HOCl in human plasma

Plasma was isolated from whole blood collected in heparinized tubes from healthy individuals. All procedures were approved by Institutional Review Board at Wayne State University. Briefly, blood samples were centrifuged at 10,000 g for 15 minutes at 4 °C. After centrifugation, the clear supernatant was collected and used for experiments. 50 μL of human plasma was spiked with 25 μM of Cobl and increasing concentrations of HOCl were added and the final volume adjusted to 100 μL. The molar ratios of Cobl: HOCl in the reaction mixtures were 0, 5, 10, 20, 30, 40, 50, 60 and 100. After addition of HOCl the reaction mixture was incubated for 2 hours for the reaction to go to completion. Following which the reaction was terminated by adding methionine. Following protein precipitation with 40 % trichloroacetic acid, the reaction mixture was subjected to HPLC and liquid chromatography mass spectrometry (LC-MS) analysis.

Mass spectrometric analysis of Cobl-HOCl reaction mixture

Mass spectrometry (MS) experiments were performed using an Agilent 6410 Triple Quadrupole mass spectrometer and an Agilent 6210 high resolution TOF instrument coupled with an Agilent 1200 HPLC system (Agilent Technologies, New Castle, DE), equipped with an electrospray source. Waters symmetry (Waters Corporation, Milford, MA) C18 column (particle size 3.5 μm; 2.1 × 100 mm) was used to separate reaction products. Solvent A was H_2O with 0.1% formic acid and solvent B was acetonitrile with 0.1% formic acid. The column was equilibrated with 100% solvent A. The gradient was: 0–45% solvent B over 10

min; 45–95% solvent B over 10 min; 95% solvent B for 1 min 95–0% solvent B for 1 min; and 100% solvent A for 13 min. 5 μL of the sample was injected at a flow rate of 0.25 mL/min. Liquid chromatography electrospray ionization (LC/ESI) MS in the positive mode was performed by triple quadrupole MS instrument using the following parameters: spray voltage 4000 V, drying gas flow 10 L/min, drying gas temperature 325°C, and nebulizer pressure 40 psi. Fragmentor voltage was 300 V in MS2 scan mode. Mass range between *m/z* 300 to 1400 was scanned to obtain full scan mass spectra. LC/electrospray ionization (ESI)MS with high resolution time of flight (TOF) instrument in the positive mode was performed using the following parameters: spray voltage 3500 V, drying gas flow 10 L/min, drying gas temperature 350°C, and nebulizer pressure 40 psi. Fragmentor voltage was 150 V in full scan mode. Mass range between *m/z* 100 to 1500 was scanned to obtain full scan mass spectra. Two reference masses at *m/z* 121.050873 and *m/z* 922.009798 were used to obtain accurate mass measurement within 5 ppm.

Solution Preparation

HOCl preparation: HOCl was prepared following a slight modification of a published method [28]. Briefly, a stock solution of HOCl was prepared by adding 1 mL NaOCl solution to 40 mL of 154 mM and the pH was adjusted to around 3 by adding HCl. The concentration of active total chlorine species in solution expressed as $[HOCl]_T$ (where $[HOCl]_T = [HOCl] + [Cl_2] + [Cl_3^-] + [OCl^-]$) in 154 mM NaCl was determined by converting all the active chlorine species to OCl^- by adding a single bolus of 40 μL 5 M NaOH and measuring the concentration of OCl^-. The concentration of OCl^- was determined spectrophotometrically at 292 nm ($\varepsilon = 362\ M^{-1}\ cm^{-1}$). As HOCl is unstable, the stock solution was freshly prepared on a daily basis, stored on ice, and used within one hour of preparation. For further experimentations, dilutions were made from the stock solution using 200 mM phosphate buffer pH 7, to give working solutions of lower HOCl concentration.

Cobl preparation: Cobl stock solution was prepared by dissolving Cobl in distilled water. The concentration of Cobl stock solution was determined spectrophotometrically at 361 nm ($\varepsilon = 27.5\ mM^{-1}\ cm^{-1}$).

RESULTS

Kinetics of reaction of HOCl with Cobl

We report a kinetic study of the reaction of an isolated, well-characterized Cobl with HOCl. We first characterized HOCl binding to Cobl and its subsequent effects on its destruction. Spectrophotometric studies demonstrated that incubation of Cobl with increasing concentrations of HOCl for 2h caused ligand replacement and Cobl destruction, as judged by a remarkable shift, decrease, and flattening in the absorbance spectra (Fig. 2A). Reactions reported here were run in the dark under aerobic condition, at 25°C. The starting trace (dotted line) is the spectrum of Cobl (11 μM) prior to HOCl addition. The prominent absorbance peak centered at 360 nm with absorbance shoulders at 540 and 550 nm, indicative of intact corrin ring with CN^- as the α-axial ligand. Incubation of Cobl with lower concentration (100 μM) of HOCl for 2h caused a distinct shift in UV absorption peak (from 360 to 363 nm), and an additional shift in the visible absorption region from (550 to 590 nm). This distinct red shift of the absorbance spectra was indicative of α-axial ligand replacement, as reported earlier [29]. Incubation of Cobl with higher concentration (>100 μM) of HOCl caused decrease and flattening in the absorbance spectra indicating oxidative destruction of the corrin ring. Traces 1–7 of Fig. 2A (solid line from top to bottom) are the end point spectra recorded after incubating identical amounts of Cobl with 100, 200, 300, 400, 500, 600, 1000 μM of HOCl for 2 hours.

We next utilized stopped-flow kinetic techniques to elucidate the mechanism by which HOCl mediated ligand replacement and corrin ring destruction. The time courses for the ligand replacement and the corrin ring destruction monitored at 363 and 590 nm were very similar. Each had a distinctive lag phase followed by an increase in absorbance which reaches a maximum intensity in less than 60 s and then decays over a period of approximately 200 min when a solution of 11 μM of Cobl was rapidly mixed with fixed HOCl concentration of 1000 μM, at 25°C (Fig. 2B). The time course for this reaction was fitted to Eq. 2 with values of k_1 and k_2 of 0.24 and 0.11 s^{-1}, respectively. The lag phase at the start of the reaction can be attributed to Cobl conformational change or perhaps the ionization of bond 5,6- dimethylbenzimidazole group, which partially limits the rate of axial ligand replacement. These experiments were conducted with fixed amount of Cobl versus increasing concentration of HOCl. The conformational change, corresponding to the lag phase, displays similar spectral characteristics to the native Cobl. The subsequent increase in absorbance that takes place in the next 60 s can be attributed to the axial ligand (either CN^- or 5,6- dimethylbenzimidazole) replacement of the Cobl molecule. Fitting each stopped flow traces obtained as a function of HOCl concentration to a two-exponential function (Eq. 2) showed that there was a variation in the observed rate constants. As shown in Fig 3A, the rate of both phases increased exponentially when plotted as a function of HOCl concentration. These characteristic slow rates at low HOCl levels may indicate that axial ligands of Cobl significantly restrict the access of HOCl to the corrin catalytic site. The parallel exponential increase in both the fast and slow rate constants may indicate that the ligand replacement rate is limited by the rate of the conformational change. Fig. 2C shows the decrease in absorbance at 590 nm that take place during the next 200 min of the reaction when increasing concentration of HOCl were rapidly mixed with a fixed concentration of Cobl (11 μM). This absorbance decrease can be attributed to Cobl destruction. The variation of the pseudo-first-order rate constant with the final HOCl concentration was linear, and the plot intersected the axes near the origin (Fig. 3B). Therefore, Cobl destruction mediated by HOCl is essentially irreversible. The second-order rate constant for the Cobl destruction estimated from the slope is found to be 2×10^{-5} $\mu M^{-1}s^{-1}$.

Liberation of CNCl from Cobl after HOCl treatment

To confirm our results from the spectrophotometric and kinetic studies, that Cobl interaction with HOCl leads to ligand substitution and corrin ring destruction, we hypothesized that the liberated CN^- will react with excess HOCl in the reaction mixture to form CNCl. Cobl (110 μM) was treated with different molar ratios of HOCl and the accumulation of CNCl as a function of increasing molar ratios of HOCl to Cobl was measured using the pyridine-1,3 dimethyl barbituric acid colorimetric assay (see *Materials and Methods* for details) (Fig. 4). From the plot it can be seen that there is an initial lag phase in the amount of CNCl being formed (up to 3.5:1 HOCl:Cobl ratio) beyond which the CNCl concentration increases linearly and plateaus of above 28:1 HOCl:Cobl ratio (Fig. 4), suggesting that 28 molecules of HOCl are required to completely destroy 1 molecule of Cobl and release CNCl.

HPLC analysis of Cobl-HOCl reaction

Fig. S1 shows the chromatograms of Cobl treated with increasing molar ratios of HOCl. Under our experimental condition Cobl eluted around 9 minutes and was identified by its characteristic spectral peaks at 360, 520 and 545 nm obtained from the diode array detector. As the HOCl concentration was increased, formation of new products with different retention times and spectral properties were seen. As shown in Fig. S1, when Cobl was treated with 3.4 times excess of HOCl there was a significant decrease in the signal for Cobl and concomitant formation of six new products with spectral characteristics similar to those of incomplete corrinoids as reported earlier [30]. Around 10 min and 13 min we observed two species with spectral characteristics very similar to that observed from the stopped-flow

kinetic experiment. Therefore, we propose these two compounds might be two stereosiomers of the α-axial ligand replaced form of the parent Cobl molecule. When HOCl concentration was further increased, all the incomplete corrinoids disappeared and only the α-axial ligand replaced form persisted. Finally, at higher concentration (> 60 fold excess of HOCl) there was complete destruction of the corrin ring as evidenced from the disappearance of the peaks. From these experiments we conclude that Cobl interacts with HOCl to undergo ligand replacement in its α-axial position, which ultimately leads to corrin destruction.

LC-MS analysis of Cobl-HOCl reaction products

LC-MS studies with different molar ratios of HOCl:Cobl reaction mixture were performed to identify the corrin degradation products. At lower HOCl concentration predominantly intact Cobl was detected (*m/z* 1355, Fig 5). Another form of Cobl *m/z* 1354 was detected with the corrin ring and the α-axial ligand intact but where the coordination between the Co atom and the N atom of the 5-6 dimethylbenzimidazole has been disrupted (Fig. 5). At higher HOCl concentration a chlorinated derivative of Cobl was detected from the characteristic chlorination isotope pattern, *m/z* 1389 (Fig. 5). The structure of this chlorinated complex reveals a ligand replacement on the α-axial side of the molecule as indicated from the spectrophotometric and HPLC analyses. The two axial ligands of the central Co atom are CN^- and Cl^-, with the phopshonucleotide moiety still intact, but not coordinated to the Co atom. Further oxidative modification of the m/z 1389 product leads to the formation of *m/z* 279 (Fig. 6). Ultimately at higher HOCl concentrations a corrin degradation product was detected which resulted from the oxidative cleavage of the carbon-carbon double bond, m/z 579 (Fig. 6).

Reaction of Cobl with HOCl in human plasma

We studied the reaction between HOCl and Cobl in human plasma utilizing both HPLC and LC-MS analysis. Human plasma (50 μL) was spiked with 25 μM of Cobl and different molar ratios of HOCl (5 to 100 fold) were added and the final volume adjusted to 100 μL. The reaction mixtures were incubated for 2 hr for reaction completion. The reactions were then terminated by adding methionine and HPLC analysis were performed following trichloroacetic acid precipitation to remove proteins. The HPLC chromatograms, at 360 nm, showed similar trends to that when Cobl were treated with HOCl in phosphate buffer solution. Furthermore LC-MS analysis revealed that all of the four molecular ions, (*m/z* 1355, 1354, 1389 and 279) (see Fig. 5 and 6) were detected when Cobl was treated with HOCl in plasma. These studies show that although HOCl has multitude of potential targets in plasma, this chemistry is still operative and indicates the biological relevance of our findings.

DISCUSSION

Our central finding is that HOCl nonenzymatically mediates Cobl destruction and subsequent liberation of toxic CNCl. This was independently demonstrated by using direct spectrophotometric and rapid kinetic measurements as well as colorimetric assay to monitor: axial ligand replacement and the corrin ring destruction; the degree of oxidation and destruction of the corrin ring; and the liberation of CNCl.

Our results demonstrate for the first time the significant role of HOCl in disturbing the stability of Cobl. The UV-visible spectrum of Cobl is extremely sensitive to ligand replacement of both α- and β-axial ligands. For example, a significant blue shifted UV-visible spectrum was produced upon the replacement of the β-axial ligand with different substituent (e.g. H_2O, CH_3, adenosyl and OH) [31–34] whereas a significant red shifted spectrum resulted upon the replacement of the dimethylbenzimidazole group attached to α-

axial with different substituent (e.g. CN^-) [29]. Despite the high affinity of HOCl towards CN^- ($k_{on} = 1.22\times10^9\ M^{-1}s^{-1}$, at 25° C) [15], the present results failed to demonstrate a direct CN^- removal prior to the corrin ring destruction. This conclusion is strongly supported by the high affinity of Co central towards CN molecule, which prevents the accessibility of HOCl to the β-axial position. Instead, HOCl-mediates the breakage and replacement of the α-axial ligand as judged by the redshifted spectral displacement when a low concentration of HOCl was added to Cobl (Fig. 2). This new species was predominant at low HOCl concentration and its accumulation was decreased by increasing HOCl concentration, and completely disappears at higher HOCl concentration (see Fig. S1). The corrin ring destruction seems to account for the complete loss and flattening of the absorbance spectrum. Changes in the corrin ring geometry upon alteration in oxidation state of the Co atom or by the replacement of the axial ligands might therefore make the ring more susceptible to HOCl-mediated oxidation and destruction. Corrin ring opening and/or destruction was associated with a significant Co release and liberation of CNCl. The lag phase that was observed in Fig. 4 could be attributed to minimum concentration of HOCl that is required for ligand replacement prior to corrin destruction. This is consistent with the HPLC analysis (Fig. S1) which shows significant accumulation of the chlorinated metabolite at 3.4:1 HOCl:Cobl ratio.

Insights into mechanisms for HOCl binding to Cobl and novel mode of Cobl destruction may provide important clues towards understanding the catalytic action of MPO at sites of inflammation. Using spectral and rapid kinetic measurements, we showed that molecular HOCl binds to Cobl through a distinct and novel mechanism. Rather than occurring through a simple, reversible one step mechanism, as is typical for HOCl binding to ferric hemoproteins [24], the reaction involves several kinetically and spectrophotometrically distinguishable marks. Single wavelength stopped-flow measurements revealed that the interaction of HOCl with Cobl consists of at least three elementary steps. The spectral changes at 363 nm over time reveals the presence of a lag phase with the kinetic tracing over the initial 5s of reaction, followed by an increase in absorbance in the next 5s, and a decrease in the absorbance over the next few hours. During the lag phase interval, the coordination environment of the metal center does not change, thus making reasonable the assumption that this step is associated with weakening and the release of the α-axial ligand. This permits the α-axial ligand replacement leading to the formation of a new hexa-coordinated intermediate. This process is illustrated by the increase in absorbance following the lag phase monitored at 363 nm. An identified intermediate with *m/z* value of 1389 is an example, where the intact nucleotide loop is still attached to the corrin ring but is not coordinated to the Co atom instead Cl atom is bound to α-axial position. Kinetic traces for the formation of the chlorinated intermediate as a function of HOCl concentration were best fitted to a two exponential function (Fig. 2B). As shown in Fig. 3A, the dependence of the pseudo-first-order rate constants of both phases on the concentration of HOCl are noticeably curved indicating that the reaction order of this substitution reaction in Cobl is higher than 1. In fact, there are second order in the HOCl concentration and the reactions follow the rate expression ($k_{obs} = k_1[HOCl]^2$) with second order rate constants of the first and second phase of $1 \times 10^{-7}\ \mu M^{-2}s^{-1}$ and $3 \times 10^{-7}\ \mu M^{-2}s^{-1}$, respectively. On the basis of the similar trends and close proximity of the value of the rate constants for the first and second steps, we concluded that the chlorinated intermediate is generated through two consecutive steps as shown in Scheme 1.

Our data clearly showed that α-axial ligand replacement initiates corrin ring destruction and the release and fragmentation of the 5,6 dimethylbenzimidazole group. The oxidation of Cobl by a slight excess of HOCl was accompanied by a remarkable change from red color to colorless. The disappearance of Cobl spectra could be due to the loss of hyperconjugation in the molecule, Co atom release, and/or Cobl fragmentation. The rate constant of Cobl

destruction obtained by fitting the decrease in absorbance monitored at 363 nm to a one exponential function is relatively slow with a positive slope (2×10^{-5} $\mu M^{-1}s^{-1}$) obtained when HOCl concentration was plotted against observed rate constant. The second order rate constant of HOCl mediated Cobl corrin ring destruction is comparable to the rate constants of HOCl with C=C in lipid molecules, adenine mononucleotide phosphate and backbone amides in protein chains (for a detailed review see [6, 35]). This similarity of the rate constants of HOCl with Cobl and other biomolecules indicated that HOCl can destroy Cobl in a complex biological mixture. Indeed, when Cobl was treated with HOCl in plasma, all the four molecular ions which were observed in the phosphate buffer reaction mixture was detected. These findings show that although HOCl has multitude of potential targets in plasma it is still capable of destroying Cobl indicating the biological relevance of our finding. The zero y-intercept confirms the irreversible nature of the reaction. The severity of Cobl destruction as assessed by the number and chain lengths of the various oxidative metabolites and subsequent buildup of CNCl is HOCl concentration dependent. The current work extends our recent work that showed the ability of HOCl to mediate the destruction of metal-ion derivatives of tetrapyrrole macrocyclic rings and their significant role in HOCl scavenging.

A proposed chemical mechanism that describes the modification and fragmentation of Cobl is shown in Scheme II. In this model, HOCl first oxidized the tertiary alcohol group in the furanose molecule of the 5,6 dimethylbenzimidazole ligand to a ketone. This reaction proceeds through the attack of the ClO_3^- anion generated from OCl^- ($3OCl^- \rightarrow ClO_3^- + 2Cl^-$) [36]. The H atom of the tertiary alcohol group forms a hydrogen bond with the adjacent O^- of the phosphate moiety to form a stable 6 membered ring. The reaction mechanism is analogous to oxidation of alcohols by Dess–Martin periodinane reagent [37, 38]. However, the higher stability of this six membered ring favors the oxidation of the tertiray alcohol as opposed to the primary alcohol of the furanose molecule. In this reaction, ClO_3^- is added onto the O atom on the phosphate group which occurs by donation of the lone pair of the O atom to the Cl atom of ClO_3^-. In the next step, a proton is exchanged with the solvent and following intamolecular electron rearrangement (as shown in Scheme 2), the alcohol group is oxidized to a ketone. Simultaneously with this oxidation there is a breakage or weakening of the coordination between Co and the N of the 5,6 dimethylbenzimidazole, leading to a ‘base-off’ conformation of the molecule. This molecule with a molecular weight of 1353 was identified in LC-MS as *m/z* 1354 in the electrospray positive mode. The *m/z* 1354 compound then undergoes a ligand replacement where a Cl^-, generated from OCl^- (as mentioned above) binds to α-axial side of the structure. This chlorinated derivative is identified as *m/z* 1389 in LC-MS, with a distinct chlorine isotope pattern. Subsequent to the ligand replacement reaction there is a cleavage of the phosphate group (through a simple acid hydrolysis as shown in Scheme 2A) of the 5,6 dimethylbenzimidazole moiety (identified as *m/z* 359) leading to the removal of this phosphonucleotide from the Cobl molecule. Additionally, there was oxidative cleavage of the corrin ring, as described previously [24, 25] which leads to the formation of di-corrinic derivative identified as *m/z* 579. The phosphonucleotide moiety that was cleaved from the Cobl molecule underwent further oxidative modification. Initially the hydroxide group (liberated from homolytic cleavge of the HOCl molecule) attacked the H atom of the five membered ring (as shown in the scheme) and eliminate the H as a water molecule. This led to the formation of a benzyl radical, from which the electron on the carbon atom attacked the bond between the esterifed O and the carbon chain. In the next step through further attack of another molecule of HOCl and subsequent intramolecular electron rearrangement, the phosphate group is released with the formation of an tertiary carbonyl group on the five membered carbon ring. The dephosphorylated moiety undergoes further oxidative modifications to form a demethylated epoxide compound, *m/z* 279 through a mechanism as shown in Scheme 2B. Based on previously published mechanisms of HOCl’s reaction with carbon-carbon double bonds, any

of the three double bonds in the six membered ring could form an epoxide. Also, any of the two methyl groups can potentally get demethylated by HOCl as shown in our mechanism. Since the structure of the *m/z* 279 is only based on mass analysis, the exact location of the epoxide and the demethylation remains to be clarified. Thus, Cobl is a potent scavenger of HOCl as evident from our finding that one molecule of Cobl has the potential capacity to scavenge multiple molecules of HOCl. The cobalt moiety of hydroxycobalamine avidly binds to intracellular cyanide (with greater affinity than cytochrome oxidase) forming cyanocobalamin. This molecule is stable, with few side effects, and is readily excreted in the urine. Therefore, hydroxycobalamine has been used to treat cyanide poisoning in clinical settings [39, 40].

However, acute or chronic inflammation can potentially lead to excess HOCl in inflammatory microenvironment where the antioxidant defenses are overwhelmed. In this scenario, the interaction of HOCl with Cobl can lead to localized toxic effects. The potential causes of the toxicity of HOCl-Cobl interaction could be related to: the release of free Co that may initiate an immunologic reaction in hypoxic and inflammatory states [41]; and the release of $CNCl/CN^{-}$ that can lead to the inhibition of mitochondrial cytochrome oxidase [18]. A recent study has demonstrated that reactive oxygen species like superoxide can be scavenged by intracellular Cobl when antioxidant defenses are overwhelmed [42]. Free Co might reduce molecular oxygen to cobalt bound oxygen radical adduct having strong oxidant properties [44]. It may also take part in Fenton-like reactions and produce hydroxyl radical ($^{\cdot}OH$) in the presence of superoxide dismutase (SOD) and hydrogen peroxide (H_2O_2) at sites of inflammation [44]. Cobalt has also been demonstrated to initiate reactive oxygen species in cancer cells and brain tissues and affect proliferation and cause DNA damage[44]. Cyanogen chloride is a colorless-to-pale yellow liquid that turns into a gas near room temperature. This reagent is a highly toxic chemical asphyxiant affecting mitochondrial respiration. Thus, supplementation with a HOCl scavenger may provide a beneficiary effect through prevention of the formation of CNCl. Indeed, previous studies by Matthews have shown that treatment of HL60 cells (cells expressing MPO) by Cobl led to cytotoxicity, which could be prevented by adding methionine, a potent scavenger of HOCl, to the medium [45].

Multiple lines of evidence suggest that MPO may play a role in atherogenesis, lung disorders and various types of cancer. For example, immunohistochemical and biochemical analyses showed the enzyme and its oxidation products to be localized within human atherosclerotic lesions [46] and ovarian cancer cells [47]. HOCl–mediated Cobl destruction may also exert indirect cardiovascular effects through its ability to disrupt the conversion of homocysteine /folic acid to methionine. Thus, enhanced levels of HOCl may lead to increased serum levels of homocysteine, a risk factor for cardiovascular disease [48]. HOCl-mediated Cobl destruction may also disturb the conversion of methylmalonic acid to succinyl-CoA [49], an input to the citric acid cycle [50, 51]. Previously, we have shown that MPO may serve as a source of free iron under oxidative stress when both NO and $O_2^{\bullet -}$ are elevated [52]. It has also been shown that iron accumulates in atherosclerotic lesions in a catalytically active form. More recently, we have shown that HOCl can promote heme destruction in free heme, hemoproteins, and red blood cells leading to iron release and protein aggregation [24]. Our work, thus, provide some exciting evidence to support the relationship between elevated levels of free metals and elevated activity of MPO. The role of MPO in the destruction of tetrapyrrole macrocyclic rings and the release of free metals may provide an additional pathway for the involvement of MPO in lipoprotein oxidation *in vivo* [53].

Therefore, inhibiting MPO and/or eliminating its final products may play a beneficiary role in biological systems in reducing the metal release mediated by HOCl. Related studies from

our lab have shown that MPO can be inhibited at three different points: 1) through heme reduction that causes collapse or narrowing in heme pocket geometry that prevents the access of the substrate to the catalytic site of the enzyme (e.g. ascorbate) [54]; 2) switching the MPO catalytic cycle from peroxidation to catalase-like activity (e.g. melatonin, tryptophan, tryptophan analogs) [55–59]; or 3) direct scavenging of HOCl (e.g. lycopene) [60].

Vitamin B12 is essential for neural function and a significant portion of elderly population is deficient in this water-soluble vitamin [61]. Our results indicate that this vitamin displays a beneficial effect in scavenging HOCl, or a harmful effect in chronic inflammatory states by destroying Cobl and generating free Co, CNCl and CN. It appears that in a system with optimal concentrations of vitamin B12, the scavenging property is well utilized, but in antioxidant deficient states, the effect of HOCl dominates and free cobalt generated in the process may add to the vicious cycle of generation of more oxidative stress.

Supplementary Material

Refer to Web version on PubMed Central for supplementary material.

Acknowledgments

This work was supported by the National Institutes of Health grant RO1 HL066367 and R01HL094230, the Children's Hospital of Michigan, the Doris Duke Foundation Clinical Scientist Development Award and the Molecular Phenotyping Core of the Michigan Nutrition and Obesity Research Center (DK089503).

ABBREVIATIONS

MPO	myeloperoxidase
H_2O_2	hydrogen peroxidase
HOCl	hypochlorus acid
CNCl	cyanogens chloride
Cobl	cyanocobalamin
HPLC	High Pressure Liquid chromatography
LC-ESI-MS	Liquid Chromatography-Electro Spray Ionization-Mass Spectrometry

References

1. Malech HL, Gallin JI. Current concepts: immunology. Neutrophils in human diseases. N Engl J Med. 1987; 317:687–694. [PubMed: 3041216]
2. Pullar JM, Vissers MC, Winterbourn CC. Living with a killer: the effects of hypochlorous acid on mammalian cells. IUBMB Life. 2000; 50:259–266. [PubMed: 11327319]
3. Kettle AJ, Winterbourn CC. Assays for the chlorination activity of myeloperoxidase. Methods Enzymol. 1994; 233:502–512. [PubMed: 8015486]
4. Weiss SJ, Klein R, Slivka A, Wei M. Chlorination of taurine by human neutrophils. Evidence for hypochlorous acid generation. J Clin Invest. 1982; 70:598–607. [PubMed: 6286728]
5. Weiss SJ. Tissue destruction by neutrophils. N Engl J Med. 1989; 320:365–376. [PubMed: 2536474]
6. Davies MJ, Hawkins CL, Pattison DI, Rees MD. Mammalian heme peroxidases: from molecular mechanisms to health implications. Antioxid Redox Signal. 2008; 10:1199–1234. [PubMed: 18331199]

7. Goud AP, Goud PT, Diamond MP, Gonik B, Abu-Soud HM. Reactive oxygen species and oocyte aging: role of superoxide, hydrogen peroxide, and hypochlorous acid. Free Radic Biol Med. 2008; 44:1295–1304. [PubMed: 18177745]
8. Vivekanadan-Giri A, Wang JH, Byun J, Pennathur S. Mass spectrometric quantification of amino acid oxidation products identifies oxidative mechanisms of diabetic end-organ damage. Rev Endocr Metab Disord. 2008; 9:275–287. [PubMed: 18752069]
9. Pennathur S, Heinecke JW. Mechanisms for oxidative stress in diabetic cardiovascular disease. Antioxid Redox Signal. 2007; 9:955–969. [PubMed: 17508917]
10. Shao B, Heinecke JW. Using tandem mass spectrometry to quantify site-specific chlorination and nitration of proteins: model system studies with high-density lipoprotein oxidized by myeloperoxidase. Methods Enzymol. 2008; 440:33–63. [PubMed: 18423210]
11. Chapman AL, Winterbourn CC, Brennan SO, Jordan TW, Kettle AJ. Characterization of non-covalent oligomers of proteins treated with hypochlorous acid. Biochem J. 2003; 375:33–40. [PubMed: 12852783]
12. Choi DK, Pennathur S, Perier C, Tieu K, Teismann P, Wu DC, Jackson-Lewis V, Vila M, Vonsattel JP, Heinecke JW, Przedborski S. Ablation of the inflammatory enzyme myeloperoxidase mitigates features of Parkinson's disease in mice. J Neurosci. 2005; 25:6594–6600. [PubMed: 16014720]
13. Pennathur S, Jackson-Lewis V, Przedborski S, Heinecke JW. Mass spectrometric quantification of 3-nitrotyrosine, ortho-tyrosine, and o,o′-dityrosine in brain tissue of 1-methyl-4-phenyl-1,2,3, 6-tetrahydropyridine-treated mice, a model of oxidative stress in Parkinson's disease. J Biol Chem. 1999; 274:34621–34628. [PubMed: 10574926]
14. Green PS, Mendez AJ, Jacob JS, Crowley JR, Growdon W, Hyman BT, Heinecke JW. Neuronal expression of myeloperoxidase is increased in Alzheimer's disease. J Neurochem. 2004; 90:724–733. [PubMed: 15255951]
15. Gerritsen CM, Margerum DW. Non-metal redox kinetics: hypochlorite and hypochlorous acid reactions with cyanide. Inorganic Chemistry. 1990; 29:2757–2762.
16. Szinicz L. History of chemical and biological warfare agents. Toxicology. 2005; 214:167–181. [PubMed: 16111798]
17. Aldridge WN. The conversion of cyanogen chloride to cyanide in the presence of blood proteins and sulphydryl compounds. Biochem J. 1951; 48:271–276. [PubMed: 14820854]
18. Turrens JF, Alexandre A, Lehninger AL. Ubisemiquinone is the electron donor for superoxide formation by complex III of heart mitochondria. Archives of Biochemistry and Biophysics. 1985; 237:408–414. [PubMed: 2983613]
19. Cadogan MP. Functional implications of vitamin B(12) deficiency. J Gerontol Nurs. 2010; 36:16–21. [PubMed: 20506933]
20. Baik HW, Russell RM. Vitamin B12 deficiency in the elderly. Annu Rev Nutr. 1999; 19:357–377. [PubMed: 10448529]
21. Varela-Moreiras G, Murphy MM, Scott JM. Cobalamin, folic acid, and homocysteine. Nutr Rev. 2009; 67(Suppl 1):S69–72. [PubMed: 19453682]
22. Ford AH, Flicker L, Alfonso H, Thomas J, Clarnette R, Martins R, Almeida OP. Vitamins B12, B6, and folic acid for cognition in older men. Neurology. 2010; 75:1540–1547. [PubMed: 20861451]
23. Banerjee R, Ragsdale SW. The many faces of vitamin B12: catalysis by cobalamin-dependent enzymes. Annu Rev Biochem. 2003; 72:209–247. [PubMed: 14527323]
24. Maitra D, Byun J, Andreana PR, Abdulhamid I, Diamond MP, Saed GM, Pennathur S, Abu-Soud HM. Reaction of hemoglobin with HOCl: Mechanism of heme destruction and free iron release. Free Radic Biol Med. 51:374–386. [PubMed: 21549834]
25. Maitra D, Byun J, Andreana PR, Abdulhamid I, Saed GM, Diamond MP, Pennathur S, Abu-Soud HM. Mechanism of hypochlorous acid-mediated heme destruction and free iron release. Free Radic Biol Med. 51:364–373. [PubMed: 21466849]
26. Lundquist P, Rosling H, Sorbo B. Determination of Cyanide in Whole-Blood, Erythrocytes, and Plasma. Clinical Chemistry. 1985; 31:591–595. [PubMed: 3978792]

27. Gumus G, Demirata B, Apak R. Simultaneous spectrophotometric determination of cyanide and thiocyanate after separation on a melamine-formaldehyde resin. Talanta. 2000; 53:305–315. [PubMed: 18968116]
28. Wang L, Bassiri M, Najafi R, Najafi K, Yang J, Khosrovi B, Hwong W, Barati E, Belisle B, Celeri C, Robson MC. Hypochlorous acid as a potential wound care agent: part I. Stabilized hypochlorous acid: a component of the inorganic armamentarium of innate immunity. J Burns Wounds. 2007; 6:e5. [PubMed: 17492050]
29. Hamza MSA, Zou X, Banka R, Brown KL, van Eldik R. Kinetic and thermodynamic studies on ligand substitution reactions and base-on/base-off equilibria of cyanoimidazolylcobamide, a vitamin B12 analog with an imidazole axial nucleoside. Dalton Transactions. 2005:782–787. [PubMed: 15702190]
30. Ford SH, Nichols A, Shambee M. The preparation and characterization of the diaquo- forms of several incomplete corrinoids: cobyric acid, cobinamide, and three isomeric cobinic acid pentaamides. J Inorg Biochem. 1991; 41:235–244. [PubMed: 2056308]
31. Wolak M, Stochel G, Hamza M, van Eldik R. Aquacobalamin (Vitamin B12a) Does Not Bind NO in Aqueous Solution. Nitrite Impurities Account for Observed Reaction. Inorganic Chemistry. 2000; 39:2018–2019. [PubMed: 12526506]
32. Fanchiang YT, Ridley WP, Wood JM. Methylation of platinum complexes by methylcobalamin. Journal of the American Chemical Society. 1979; 101:1442–1447.
33. Hogenkamp HPC. Chemical synthesis and properties of analogs of adenosylcobalamin. Biochemistry. 1974; 13:2736–2740. [PubMed: 4847542]
34. Greenberg SS, Xie J, Zatarain JM, Kapusta DR, Miller MJ. Hydroxocobalamin (vitamin B12a) prevents and reverses endotoxin-induced hypotension and mortality in rodents: role of nitric oxide. Journal of Pharmacology and Experimental Therapeutics. 1995; 273:257–265. [PubMed: 7714773]
35. Pattison DI, Davies MJ. Reactions of myeloperoxidase-derived oxidants with biological substrates: gaining chemical insight into human inflammatory diseases. Curr Med Chem. 2006; 13:3271–3290. [PubMed: 17168851]
36. Gordon G, Tachiyashiki S. Kinetics and mechanism of formation of chlorate ion from the hypochlorous acid/chlorite ion reaction at pH 6–10. Environmental Science & Technology. 1991; 25:468–474.
37. Dess DB, Martin JC. Readily accessible 12-I-5 oxidant for the conversion of primary and secondary alcohols to aldehydes and ketones. The Journal of Organic Chemistry. 1983; 48:4155–4156.
38. Meyer SD, Schreiber SL. Acceleration of the Dess-Martin Oxidation by Water. The Journal of Organic Chemistry. 1994; 59:7549–7552.
39. Forsyth JC, Mueller PD, Becker CE, Osterloh J, Benowitz NL, Rumack BH, Hall AH. Hydroxocobalamin as a cyanide antidote: safety, efficacy and pharmacokinetics in heavily smoking normal volunteers. J Toxicol Clin Toxicol. 1993; 31:277–294. [PubMed: 8492341]
40. Hall AH, Rumack BH. Hydroxycobalamin/sodium thiosulfate as a cyanide antidote. J Emerg Med. 1987; 5:115–121. [PubMed: 3295013]
41. Saini Y, Greenwood KK, Merrill C, Kim KY, Patial S, Parameswaran N, Harkema JR, LaPres JJ. Acute cobalt-induced lung injury and the role of hypoxia-inducible factor 1alpha in modulating inflammation. Toxicol Sci. 2010; 116:673–681. [PubMed: 20511350]
42. Suarez-Moreira E, Yun J, Birch CS, Williams JHH, McCaddon A, Brasch NE. Vitamin B12 and Redox Homeostasis: Cob(II)alamin Reacts with Superoxide at Rates Approaching Superoxide Dismutase (SOD). Journal of the American Chemical Society. 2009; 131:15078–15079. [PubMed: 19799418]
43. Suarez-Moreira E, Yun J, Birch CS, Williams JH, McCaddon A, Brasch NE. Vitamin B(12) and redox homeostasis: cob(II)alamin reacts with superoxide at rates approaching superoxide dismutase (SOD). J Am Chem Soc. 2009; 131:15078–15079. [PubMed: 19799418]
44. Mates JM, Segura JA, Alonso FJ, Marquez J. Roles of dioxins and heavy metals in cancer and neurological diseases using ROS-mediated mechanisms. Free Radic Biol Med. 2010; 49:1328–1341. [PubMed: 20696237]

45. Matthews JH. Cyanocobalamin [c-lactam] inhibits vitamin B12 and causes cytotoxicity in HL60 cells: methionine protects cells completely. Blood. 1997; 89:4600–4607. [PubMed: 9192785]
46. Daugherty A, Dunn JL, Rateri DL, Heinecke JW. Myeloperoxidase, a catalyst for lipoprotein oxidation, is expressed in human atherosclerotic lesions. J Clin Invest. 1994; 94:437–444. [PubMed: 8040285]
47. Saed GM, Ali-Fehmi R, Jiang ZL, Fletcher NM, Diamond MP, Abu-Soud HM, Munkarah AR. Myeloperoxidase serves as a redox switch that regulates apoptosis in epithelial ovarian cancer. Gynecol Oncol. 116:276–281. [PubMed: 19962178]
48. Wang TJ, Gona P, Larson MG, Tofler GH, Levy D, Newton-Cheh C, Jacques PF, Rifai N, Selhub J, Robins SJ, Benjamin EJ, D'Agostino RB, Vasan RS. Multiple biomarkers for the prediction of first major cardiovascular events and death. N Engl J Med. 2006; 355:2631–2639. [PubMed: 17182988]
49. Halpern J. Mechanisms of coenzyme B12-dependent rearrangements. Science. 1985; 227:869–875. [PubMed: 2857503]
50. Booß-Bavnbek, B.; Klösgen, B.; Larsen, J.; Pociot, F.; Renström, E.; Maechler, P. Mitochondria and Metabolic Signals in β-Cells. In: Choi, S., editor. BetaSys. Springer; New York: p. 53-71.
51. LaNoue KF, Bryla J, Williamson JR. Feedback Interactions in the Control of Citric Acid Cycle Activity in Rat Heart Mitochondria. Journal of Biological Chemistry. 1972; 247:667–679. [PubMed: 4333508]
52. Galijasevic S, Maitra D, Lu T, Sliskovic I, Abdulhamid I, Abu-Soud HM. Myeloperoxidase interaction with peroxynitrite: chloride deficiency and heme depletion. Free Radic Biol Med. 2009; 47:431–439. [PubMed: 19464362]
53. Nicholls SJ, Hazen SL. Myeloperoxidase, modified lipoproteins, and atherogenesis. J Lipid Res. 2009; 50(Suppl):S346–351. [PubMed: 19091698]
54. Abu-Soud HM, Hazen SL. Interrogation of heme pocket environment of mammalian peroxidases with diatomic ligands. Biochemistry. 2001; 40:10747–10755. [PubMed: 11535049]
55. Galijasevic S, Abdulhamid I, Abu-Soud HM. Melatonin is a potent inhibitor for myeloperoxidase. Biochemistry. 2008; 47:2668–2677. [PubMed: 18237195]
56. Lu T, Galijasevic S, Abdulhamid I, Abu-Soud HM. Analysis of the mechanism by which melatonin inhibits human eosinophil peroxidase. Br J Pharmacol. 2008; 154:1308–1317. [PubMed: 18516076]
57. Maitra D, Banerjee J, Shaeib F, Souza CE, Abu-Soud HM. Melatonin can mediate its vascular protective effect by modulating free iron level by inhibiting hypochlorous Acid-mediated hemoprotein heme destruction. Hypertension. 57:e22. [PubMed: 21464394]
58. Sliskovic I, Abdulhamid I, Sharma M, Abu-Soud HM. Analysis of the mechanism by which tryptophan analogs inhibit human myeloperoxidase. Free Radic Biol Med. 2009; 47:1005–1013. [PubMed: 19596067]
59. Galijasevic S, Abdulhamid I, Abu-Soud HM. Potential role of tryptophan and chloride in the inhibition of human myeloperoxidase. Free Radic Biol Med. 2008; 44:1570–1577. [PubMed: 18279680]
60. Pennathur S, Maitra D, Byun J, Sliskovic I, Abdulhamid I, Saed GM, Diamond MP, Abu-Soud HM. Potent antioxidative activity of lycopene: A potential role in scavenging hypochlorous acid. Free Radic Biol Med. 49:205–213. [PubMed: 20388538]
61. Andres E, Loukili NH, Noel E, Kaltenbach G, Abdelgheni MB, Perrin AE, Noblet-Dick M, Maloisel F, Schlienger JL, Blickle JF. Vitamin B12 (cobalamin) deficiency in elderly patients. CMAJ. 2004; 171:251–259. [PubMed: 15289425]

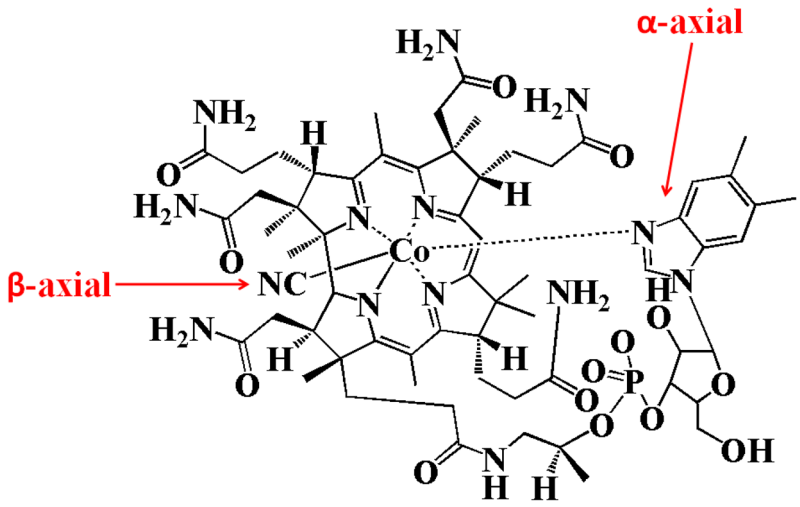

Figure 1.
Structure of cyanocobalamin.

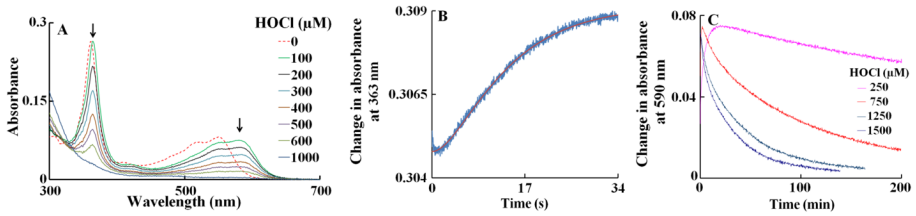

Figure 2.

UV/Vis spectral changes and kinetic analysis of Cobl-HOCl interaction. **Panel A** shows the spectral changes for concentration dependence of HOCl-mediated corrin ring destruction. The dashed line represents spectral traces of Cobl (11 μM) recorded in phosphate buffer (200 mM, pH 7), at 25°C. Spectral traces (solid lines, from top to bottom) were recorded after 2 h of incubation of a fixed amount Cobl with increasing concentration of HOCl (100, 200, 300, 400, 600 and 1000 μM), at 25°C. Arrows in the panel indicate the direction of spectral change as a function of increasing concentration of HOCl. **Panel B** shows the stopped-flow trace monitored at 363 nm when a buffer solution containing Cobl (11 μM, final) was rapidly mixed with an equal volume of buffer solution supplemented with HOCl (1000 μM, final), at 25 °C. The red line represents the theoretical fit generated by the software when the raw data (blue line) was fitted to a two exponential function (Eq. 2). **Panel C** contains the kinetic traces for the reaction monitored at 590 nm, when Cobl (11 μM) was mixed with increasing concentrations of HOCl (250, 750, 1250 and 1500 μM). These data are representative of three independent experiments.

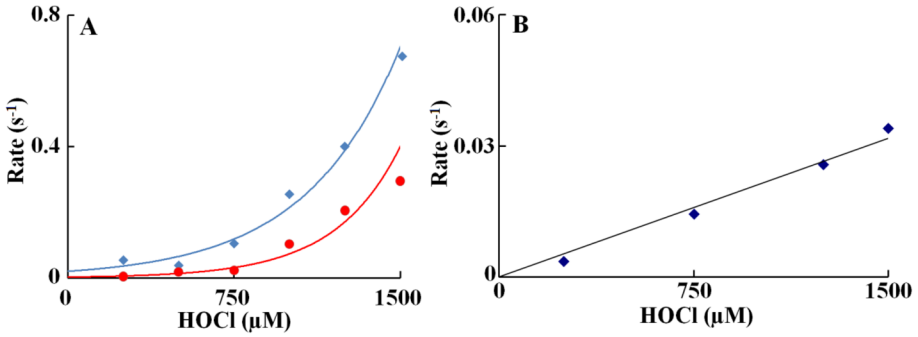

Figure 3.

Rate constant of α-axial ligand replacement and corrin ring destruction of CobI as a function of HOCl concentration. The observed rate constants for the formation of CobI intermediate upon reacting CobI with HOCl (panel A) and subsequent CobI destruction (panel B) monitored at 363 nm observed in Fig. 3 were plotted as a function of HOCl concentration. A solution containing 11 μM CobI was rapidly mixed with an equal volume of sodium phosphate buffer (200 mM, pH 7) supplemented with varying concentration of HOCl at 25 °C. The high concentration of the phosphate buffer is to keep the pH of the solution unaltered after the addition of HOCl. These data are representative of three independent experiments and the standard error for each individual rate constant has been estimated to be less than 5%.

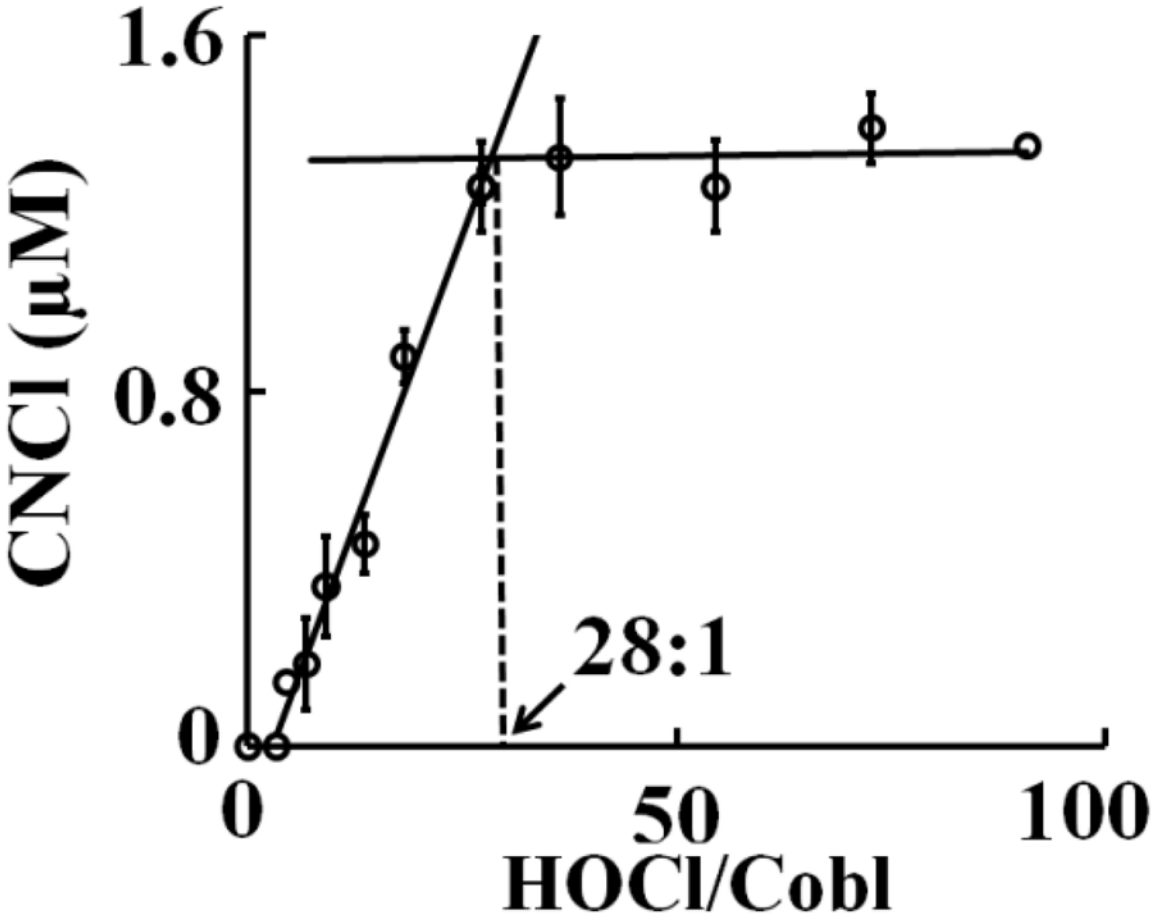

Figure 4.

Cobl destruction mediated by HOCl causes the liberation of CNCl. Cobl was treated with increasing molar ratios of HOCl:Cobl and CNCl generation was assayed colorimetrically as detailed in the *Materials and Methods* section. The data are a representative of three independent experiments with the error bars representing the standard error measurements.

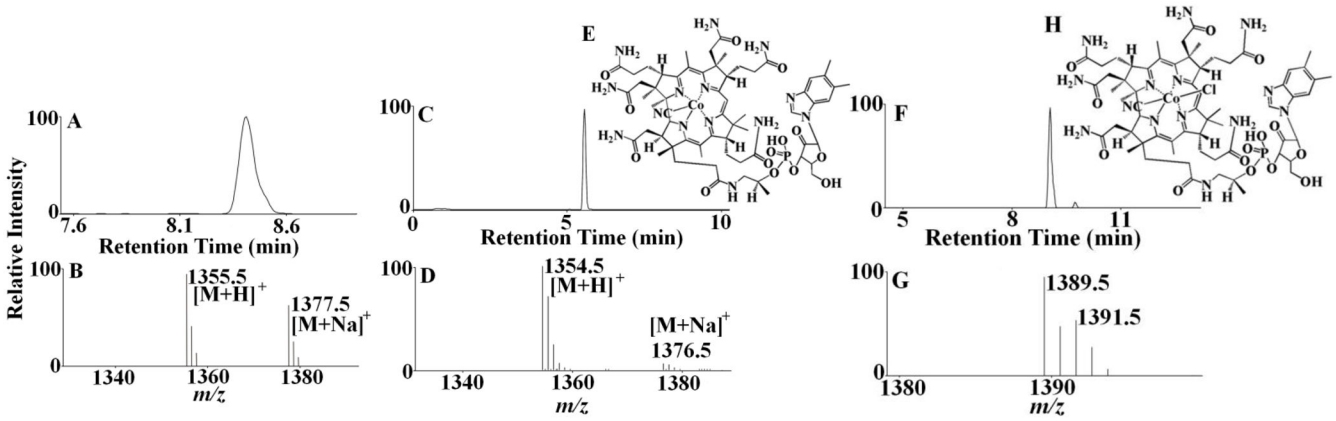

Figure 5.

Mass spectrometric detection of Cobl-HOCl reaction products. The extracted ion chromatogram (A) and MS spectrum (B) of unreacted Cobl as detected from the Cobl-HOCl reaction mixture. The molecular ion was detected in the $[M+H]^+$ form and had a *m/z* of 1355. Disruption of coordination in Cobl when reacted with HOCl formed a 'base-off' intermediate. Examination of the MS spectrum revealed that the $[M+H]^+$ ion had a *m/z* 1354. (C) The extracted ion chromatogram, (D) The MS spectrum of the peak and (E) the assigned structure of *m/z* 1354. Formation of a chlorinated derivative of Cobl on reacting with HOCl with a $[M + H]^+$ ion having a *m/z* 1389. (F) The extracted ion chromatogram, (G) the MS spectrum of the peak. Note the presence of one chlorine atom as the ion intensity of the $[M+H+2]^+$ ion is approximately 40% of $[M+H]^+$, indicating a chlorine isotope pattern. (H) The assigned structure of *m/z* 1389.

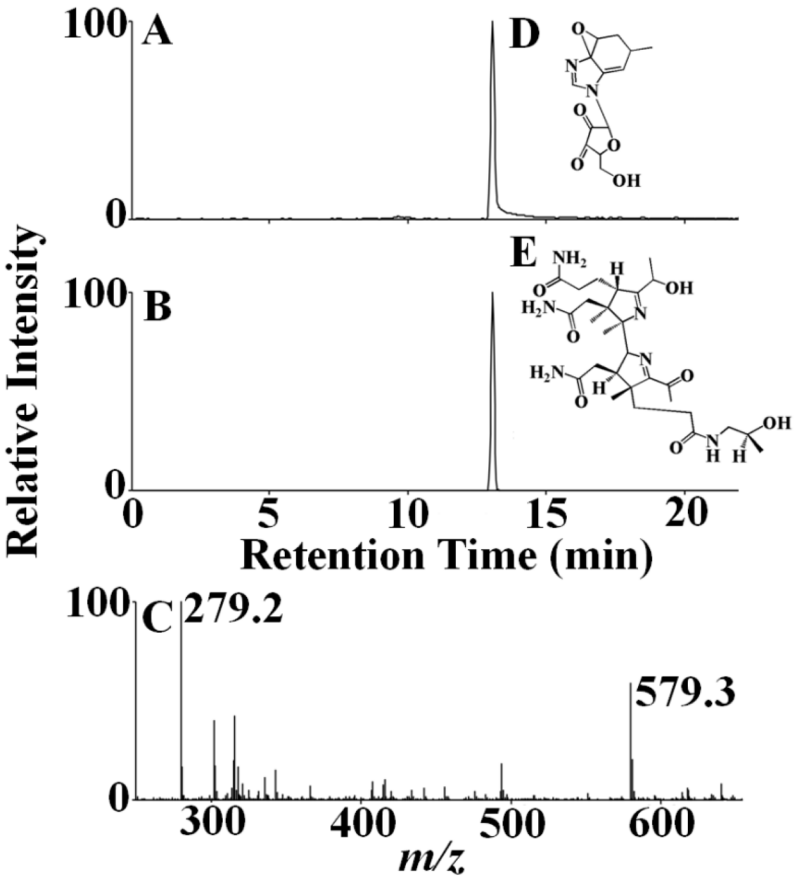

Figure 6.

Oxidative modification of the phosphonucleotide moiety and the corrin ring of Cobl. Extracted ion chromatogram (A & B) and MS spectrum (C) of oxidatively modified phosphonucleotide moiety and corrin degradation product, detected from the Cobl-HOCl reaction mixture. The molecular ion was detected in the $[M+H]^+$ form and had a *m/z* of 279 and 579. The assigned structures of *m/z* 279 and 579 are shown in D & E.

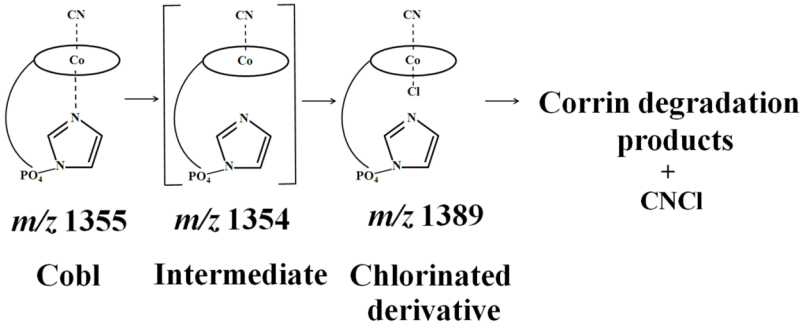

Scheme 1.

Kinetic model depicting the reaction between Cobl and HOCl leading to ligand replacement and corrin ring destruction.

A: Mechanism of ligand replacement and corrin ring clevage

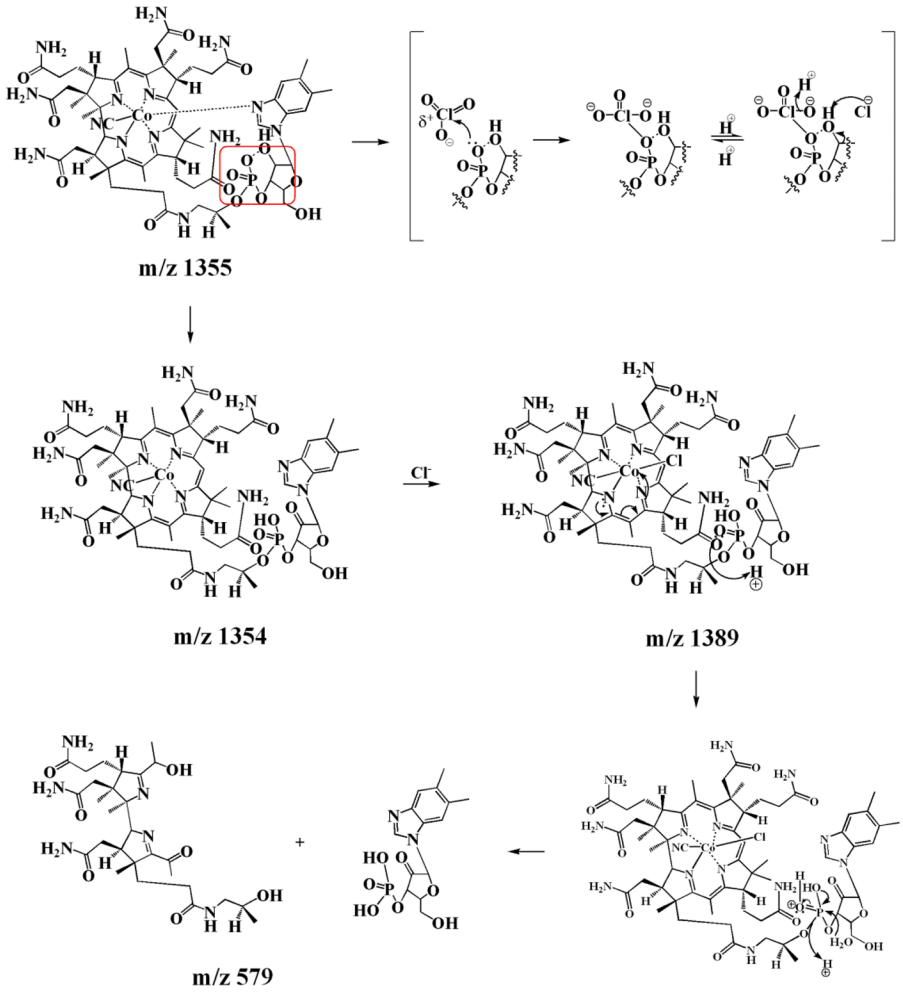

B: Mechanism of dephosphorylation and demethylation

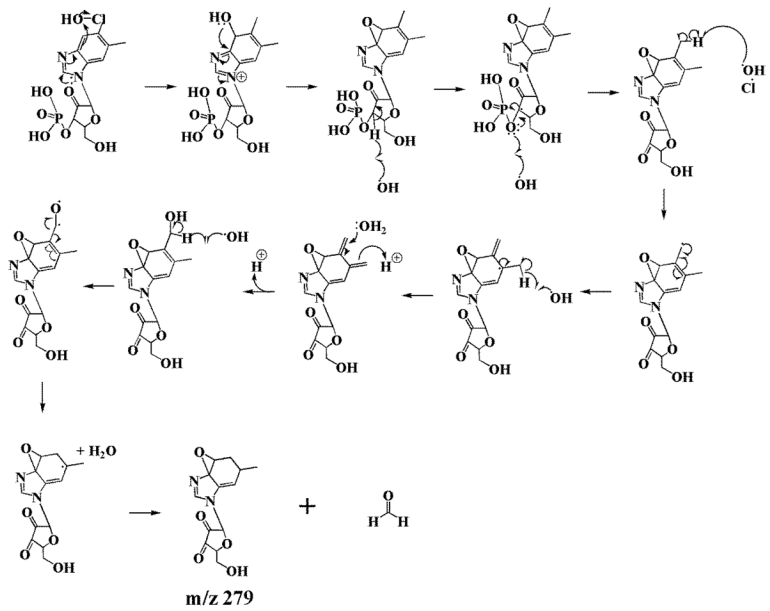

Scheme 2.

A general kinetic model explains the interaction of Cobl with HOCl leading to the axial ligand replacement, corrin ring degradation.